

**Supplementary materials**  
**for**  
**A rapid synthesis of magnetic-core mesoporous**  
**silica-shell nanostructures -as potential**  
**theranostic agents, by means of microwave**  
**irradiation and the atrane method**

**M. Dolores Garrido,<sup>1,2\*</sup> Bejan Hamawandi,<sup>2</sup> José Francisco Serrano-Claumarchirant,<sup>2</sup> Giovanni Marco Saladino,<sup>2</sup> Adem B. Ergül,<sup>2</sup> M. Dolores Marcos,<sup>3</sup> José Vicente Ros-Lis,<sup>4</sup> Pedro Amorós,<sup>1</sup> Muhammet S. Toprak<sup>2\*</sup>**

<sup>1</sup> Institut de Ciència dels Materials (ICMUV), Universitat de València, Catedrático José Beltrán 2, 46980 Paterna, Valencia (Spain)

<sup>2</sup> KTH Royal Institute of Technology, Department of Applied Physics, SE106 91 Stockholm, Sweden

<sup>3</sup> Instituto Interuniversitario de Investigación de Reconocimiento Molecular y Desarrollo Tecnológico (IDM), Universitat Politècnica de València, Valencia (Spain).

<sup>4</sup> Instituto Interuniversitario de Investigación de Reconocimiento Molecular y Desarrollo Tecnológico (IDM), Universitat de València, C/ Dr. Moliner 50, 46100 Burjassot, Valencia (Spain)

Corresponding authors: [maria.d.garrido@uv.es](mailto:maria.d.garrido@uv.es); [toprak@kth.se](mailto:toprak@kth.se)

Table S1. Synthesis parameters, hydrodynamic size – polydispersity index (pdl), and dry size (estimated from Gaussian multimodal fit) of various samples.

Sample	m (citrate) (g)	Ramping time (min)	Aging time (min)	Temperature (°C)	Hydrodynamic size (nm) / pdl	Dry size (nm) (Percentage)
A	0.454	1	10	180	-	-
B	0.454	1	10	200	-	-
C	0.454	1	10	220	246 ± 81 / 0.08	118 ± 36 (%51) 51 ± 18 (%49)
D	0.454	1	20	220	295 ± 88 / 0.25	138 ± 21 (%66) 90 ± 25 (%34)
E	0.454	1	30	220	259 ± 90 / 0.27	80 ± 36 (%21) 47 ± 16 (%79)
F	454	10	20	180	-	-
G	454	10	20	200	-	-
H	0.114	10	20	220	163 ± 67 / 0.11	117 ± 21 (%50) 74 ± 21 (%50)
I	0.227	10	20	220	255 ± 84 / 0.20	123 ± 25 (%32) 82 ± 17 (%68)
J	0.454	10	20	220	359 ± 122 / 0.14	182 ± 24 (%66) 120 ± 26 (%34)
K	0.908	10	20	220	214 ± 75 / 0.07	153 ± 30 (%30) 77 ± 22 (%70)
L	0.454	20	20	180	-	-
M	0.454	20	20	200	-	-
N	0.454	20	10	220	190 ± 85 / 0.12	141 ± 18 (%55) 113 ± 18 (%45)
O	0.454	20	20	220	410 ± 10 / 0.30	213 ± 23 (%70) 143 ± 34 (%30)
P	0.454	20	30	220	203 ± 77 / 0.12	167 ± 24 (%50) 137 ± 24 (%50)
Q	0.454	20	20	250	175 ± 68 / 0.09	125 ± 22 (%36) 93 ± 19 (%64)
R	0.908	20	20	220	175 ± 63 / 0.11	140 ± 33 (%37) 118 ± 19 (%63)

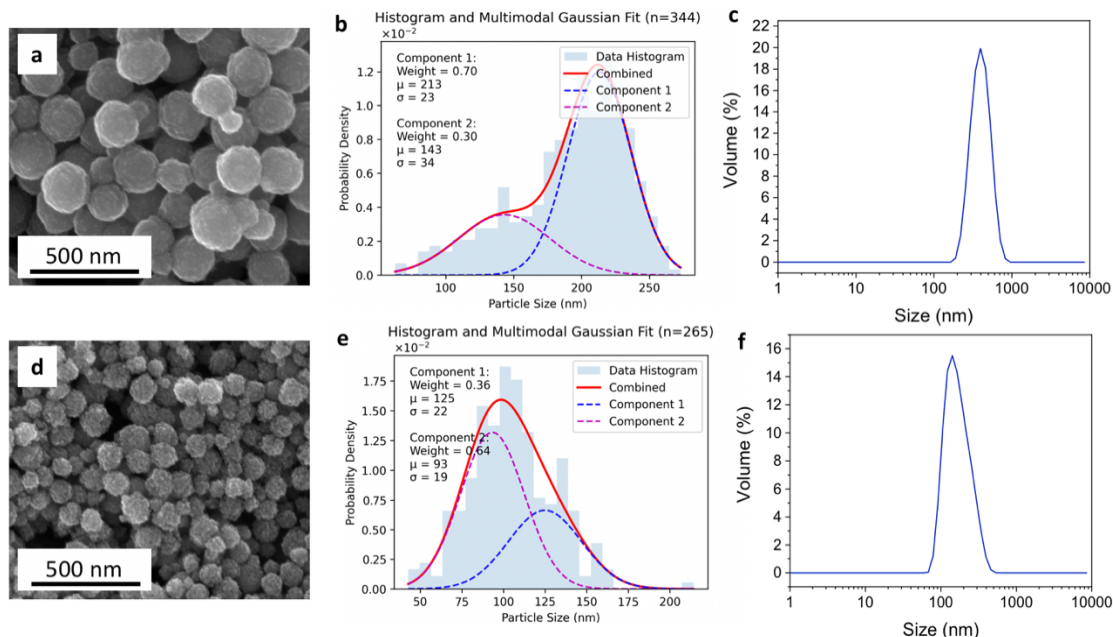


Fig. S1. SEM micrographs, particle size distribution (from SEM micrographs) with Gaussian-fits (number of particles measured are displayed above the graph), and hydrodynamic size (DLS) of the samples obtained at different reaction temperatures: (a, b, c) 220 °C (Exp O) and (d, e, f) 250 °C. (Exp Q) For further experimental details, see Table S1.

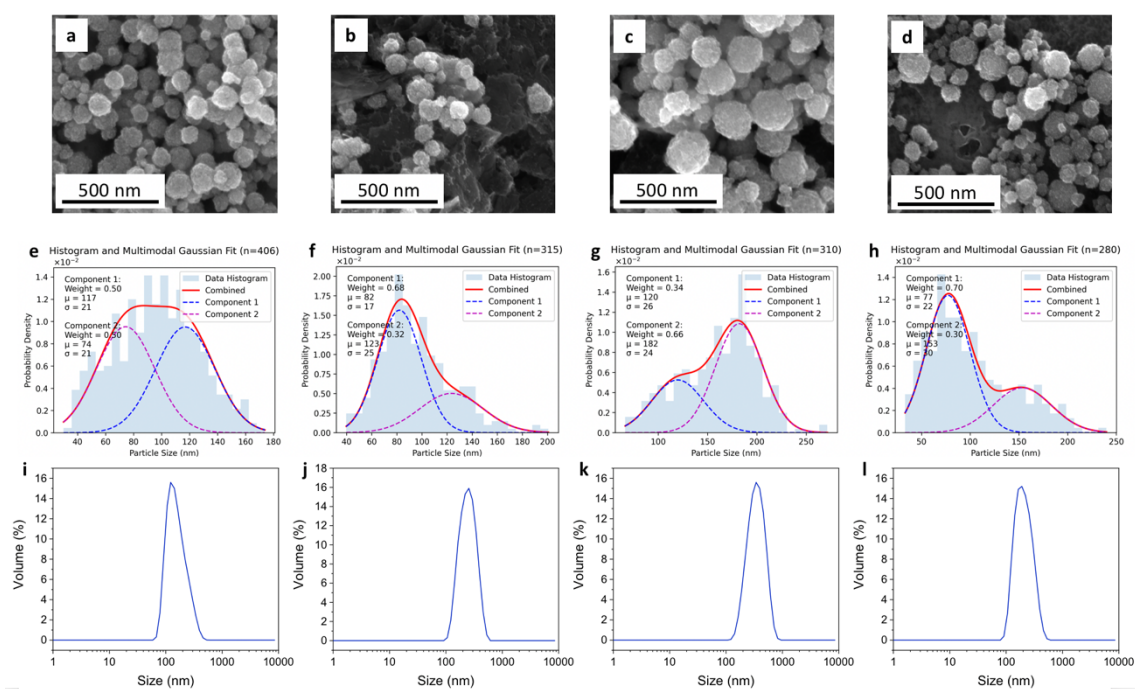


Fig. S2. SEM micrographs, particle size distribution (from SEM micrographs) with Gaussian-fits (number of particles measured are displayed above the graph), and hydrodynamic size (DLS) of the samples obtained with different citrate quantities: (a, e, i) 0.114 g (Exp F), (b, f, j) 0.227 g (Exp I), (c, g, k) 0.454 g (Exp J), and (d, h, l) 0.908 g (Exp K). For further experimental details, see Table S1.

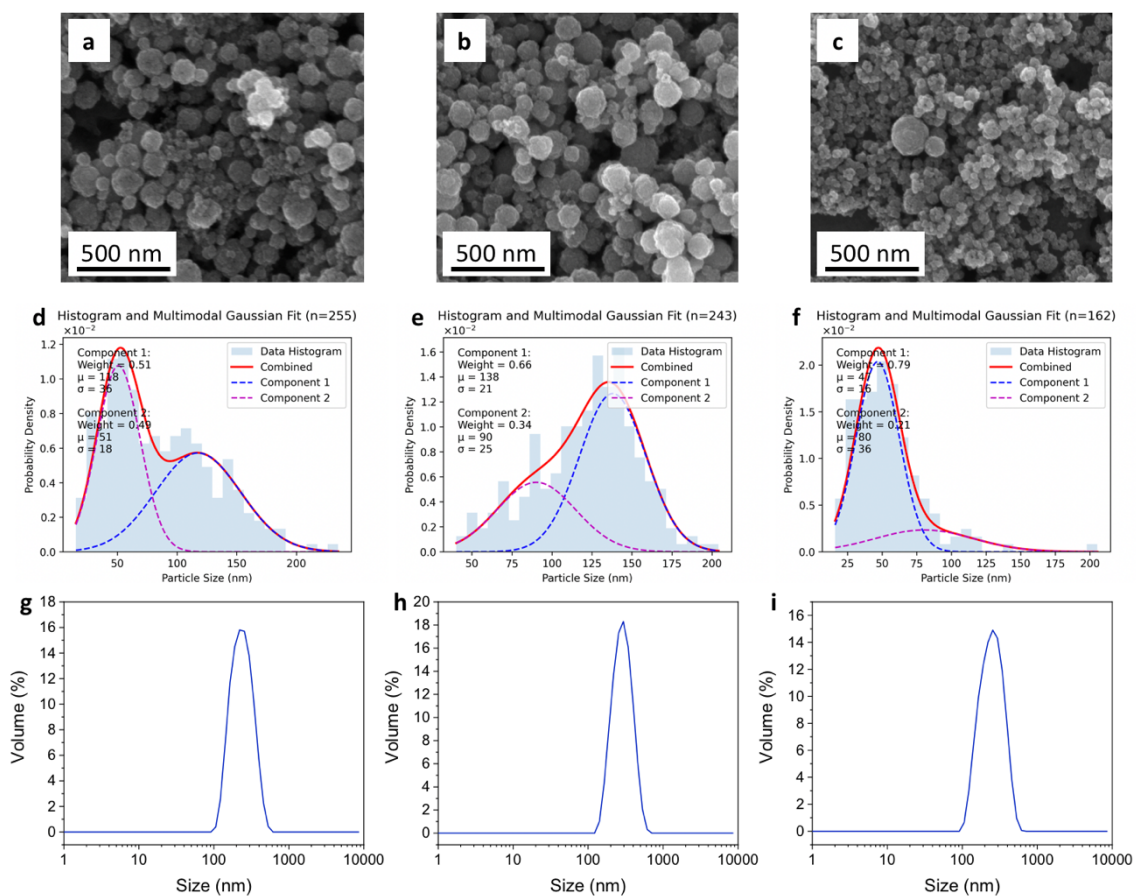


Fig. S3. SEM micrographs, particle size distribution (from SEM micrographs) with Gaussian-fits (number of particles measured are displayed above the graph), and hydrodynamic size (DLS) of the samples prepared at 220 °C with 1 min ramping at aging times of: (a, d, g) 10 min (Exp C), (b, e, h) 20 min (Exp D), and (c, f, i) 30 min (Exp E). For further experimental details, see Table S1.

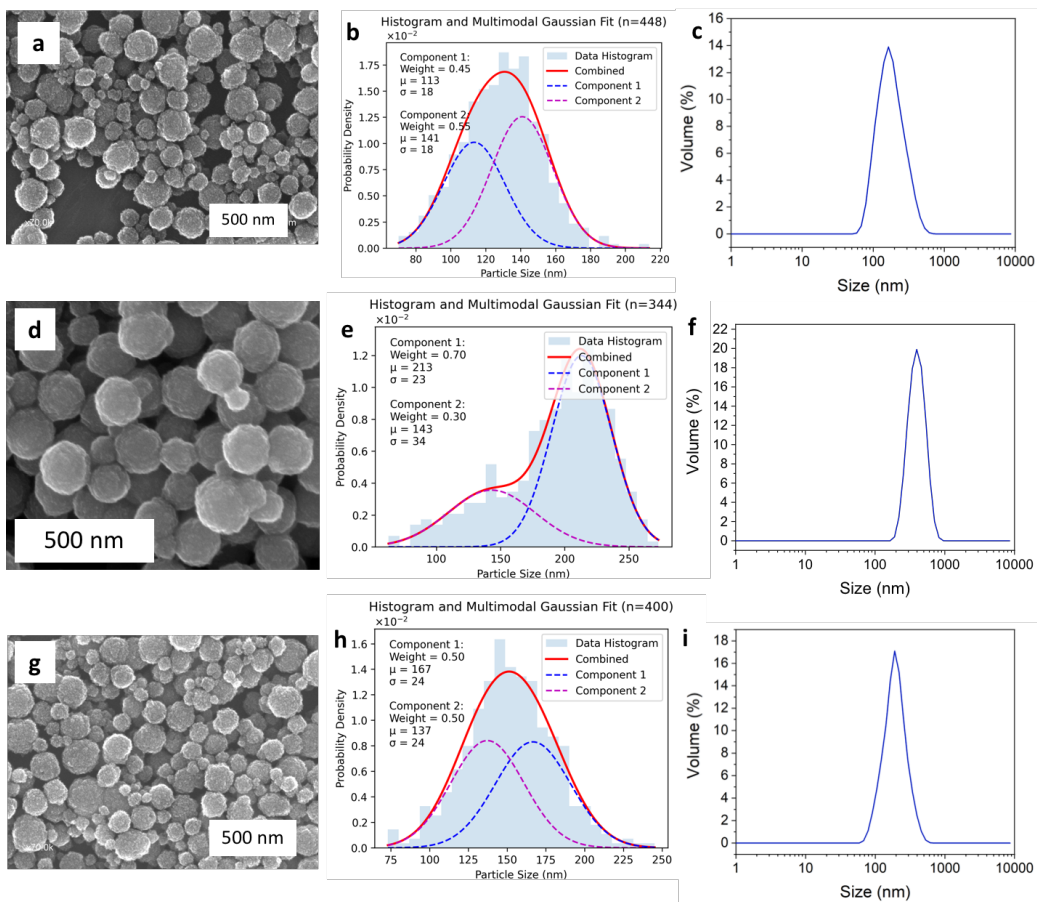


Fig. S4. SEM micrographs, particle size distribution (from SEM micrographs) with Gaussian-fits (number of particles measured are displayed above the graph), and hydrodynamic size (DLS) of the samples prepared at 220 °C with ramping time of 20 min at aging times of: (a, b,c) 10 min (Exp N), (d, e, f) 20 min (Exp O), and (g, h, i) 30 min (Exp P). For further experimental details, see Table S1.

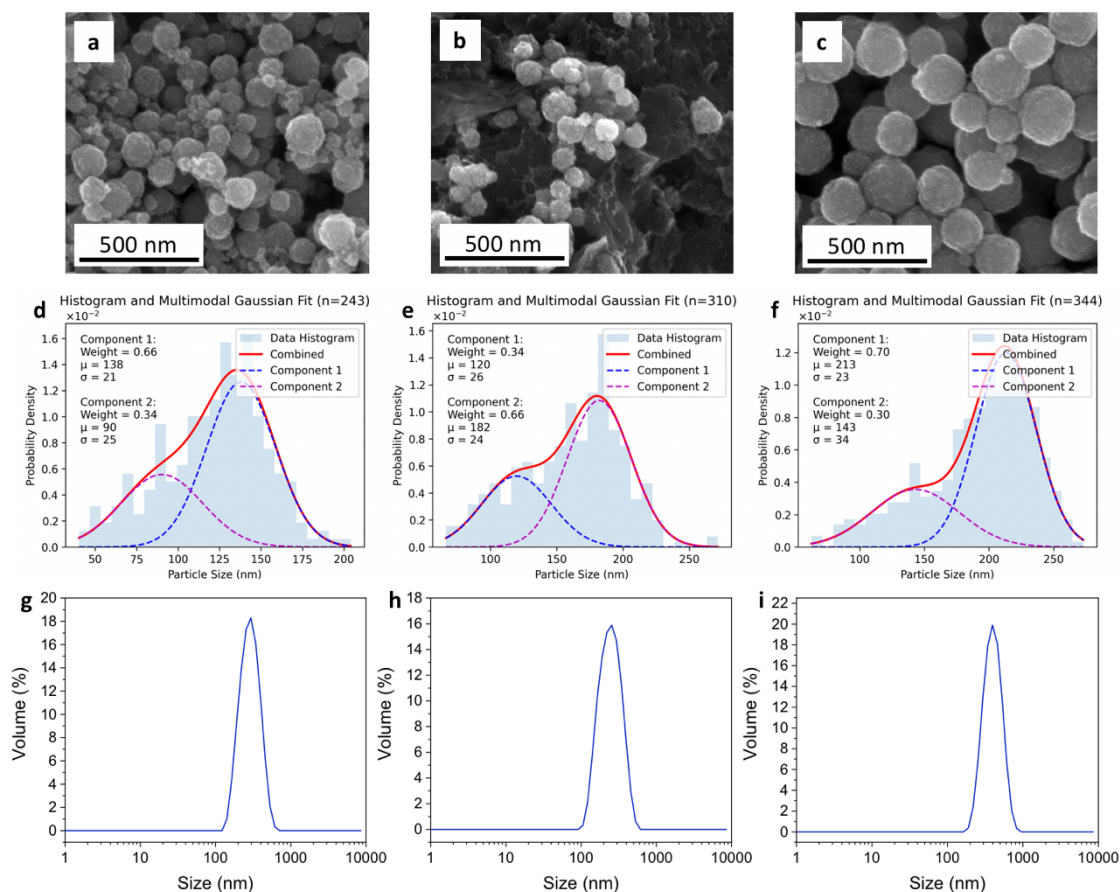


Fig. S5. SEM micrographs, particle size distribution (from SEM micrographs) with Gaussian-fits (number of particles measured are displayed above the graph), and hydrodynamic size (DLS) of the samples obtained with different ramping times: (a, d, g) 1 min (Exp D), (b, e, h) 10 min (Exp J), and (c, f, i) 20 min (Exp O). For further experimental details, see Table S1.

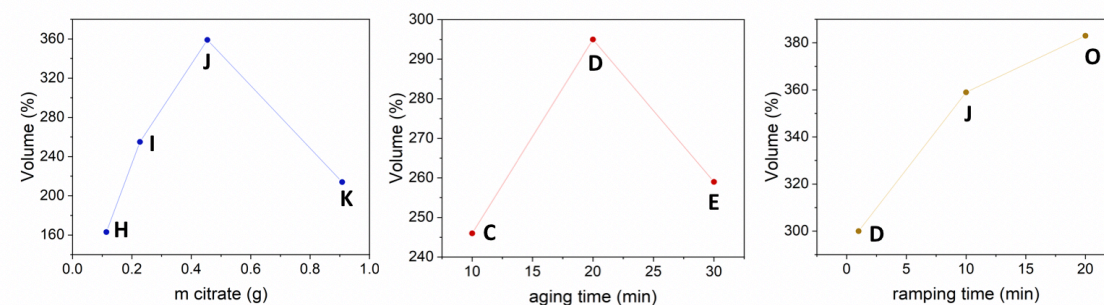


Fig. S6. Hydrodynamic size evolution of SPION-NCs, for the synthesis reactions performed at 220 °C, with different reaction parameters –with the change of one parameter at a time: (a) amount of citrate, (b) aging time, and (c) ramping time. Sample are labeled on the plots, and experimental details are summarized in Table S1.

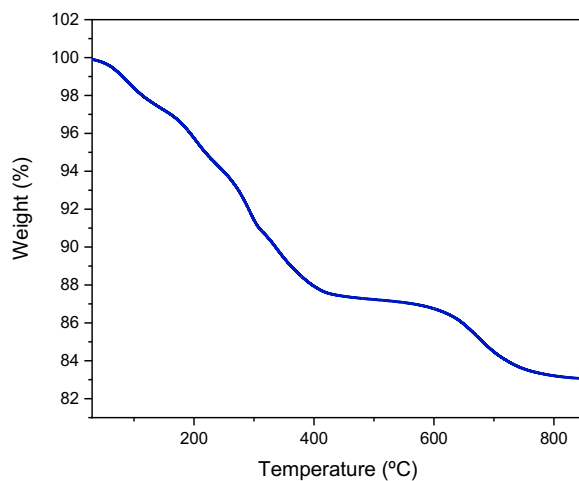


Fig. S7. TGA thermogram of SPIONs-NCs (Exp O).

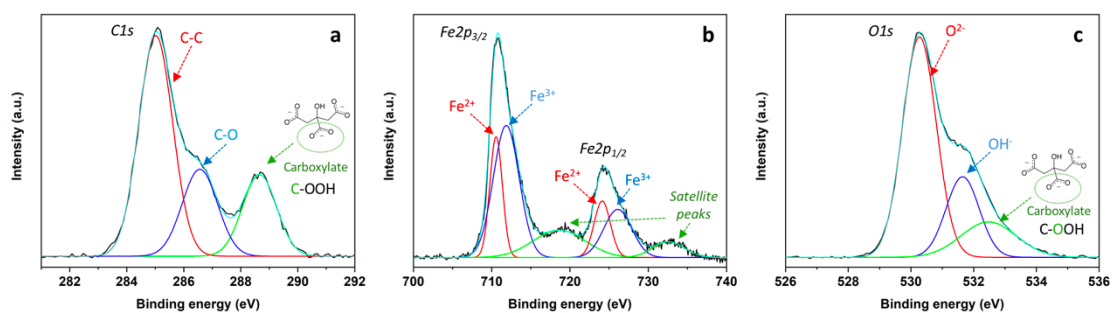


Fig. S8. XPS spectra of the SPIONs-NCs (Exp. C) (a) C 1s, (b) Fe 2p, and (c) O 2s.

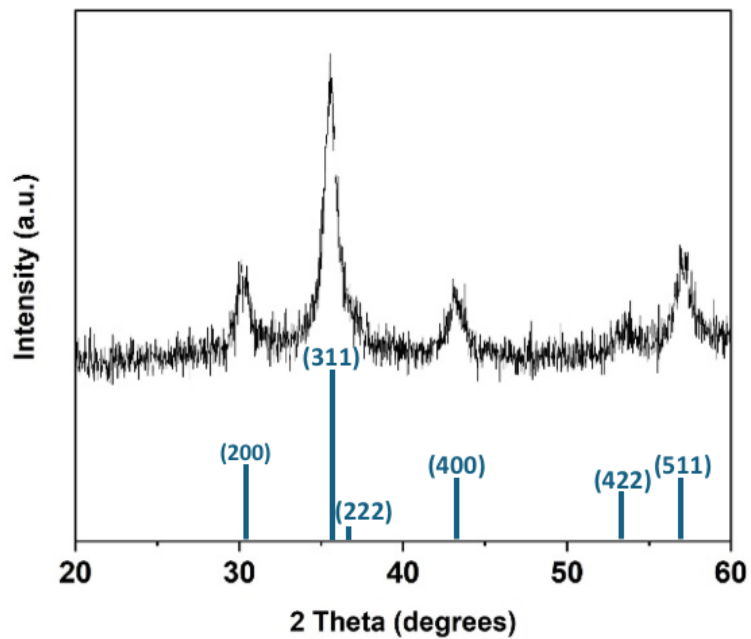


Fig. S9. XRD of the SPIONs-NCs (Exp. O), indexed to magnetite phase,  $\text{Fe}_3\text{O}_4$  (ICDD file No. 19-0629).

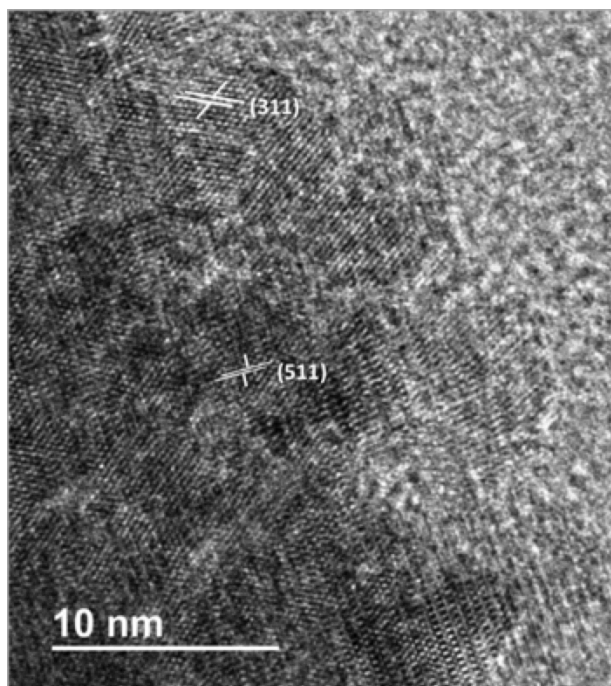


Fig S10. HRTEM of SPIONs-NCs (Exp. O). Observed crystalline planes were indexed to magnetite phase,  $\text{Fe}_3\text{O}_4$  (ICDD file No. 19-0629)

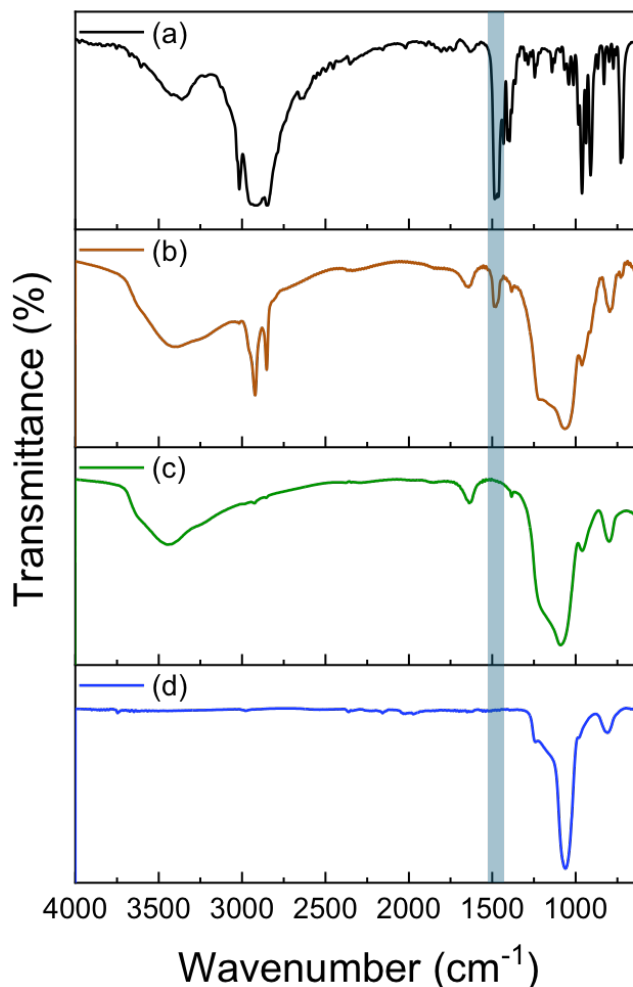


Fig. S11. FTIR spectra of (a) CTAB, (b) mesoporous silica before extraction, (c) mesoporous silica after extraction of CTAB with salt, and (d) mesoporous silica after calcination at 550 °C for 6h.

The amount of methylene blue (MB) was calculated by the difference using a calibration curve with UV-Vis (Fig. S12a). For this purpose, using UV-Vis spectroscopy a calibration curve was generated by preparing MB solutions with concentrations ranging from 0.5  $\mu\text{g/mL}$  to 7.5  $\mu\text{g/mL}$ . The area under the absorption spectrum (in the range from 550 nm till 700 nm) is integrated, as the isomers (dimer, trimer, etc.) of MB have slightly shifted absorption maxima. To determine the quantity of encapsulated MB, two stock solutions with identical MB concentration were prepared, where one was analyzed for the total amount of MB used for the impregnation process. The second solution was obtained after the impregnation, pore-closure and washing process, during which all MB not encapsulated within the pores was collected (the sample was washed repeatedly until no residual MB was observed). The total amount of free (non-encapsulated) MB was determined from the UV-Vis analysis of this solution, upon the integration of the area under the absorption curve (Fig. S12b). After interpolating the concentrations from the calibration curve for each sample, the amount of MB present within the pores of the material was determined by the difference.

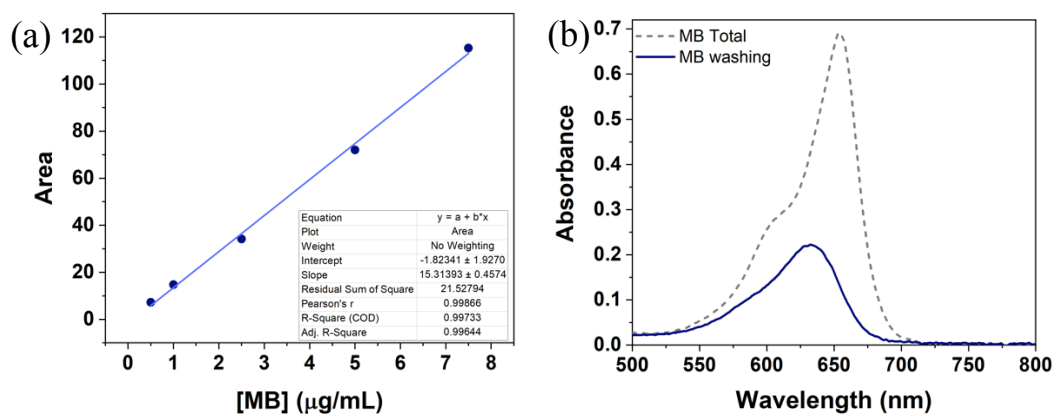


Fig. S12. (a) UV-Vis calibration curve for MB, and (b) Absorption spectrum of total MB (prior to impregnation), and MB in the supernatant after washing steps.

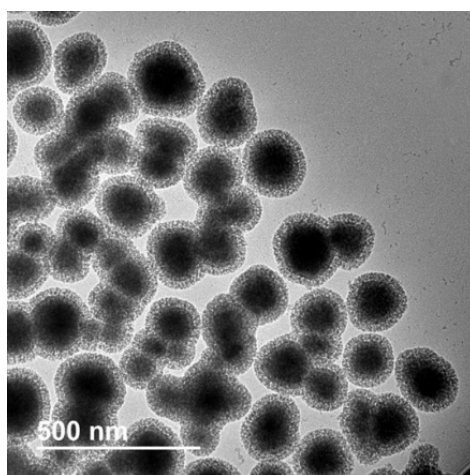


Fig. S13. TEM micrograph of SPIONs-NCs@MS-MB.

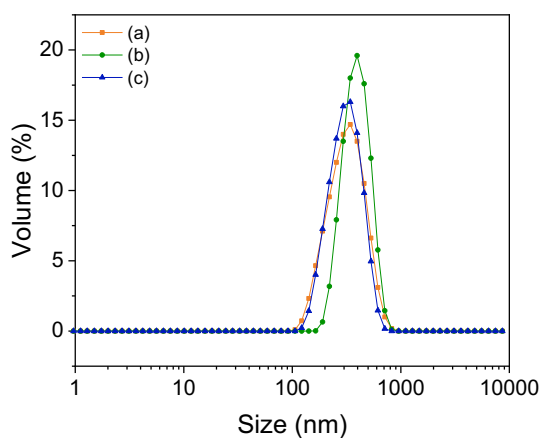


Fig. S14. Hydrodynamic size of a) SPIONs-NCs-amorphous silica, b) SPIONs-NCs@MS, and c) SPIONs-NCs@MS-MB samples.

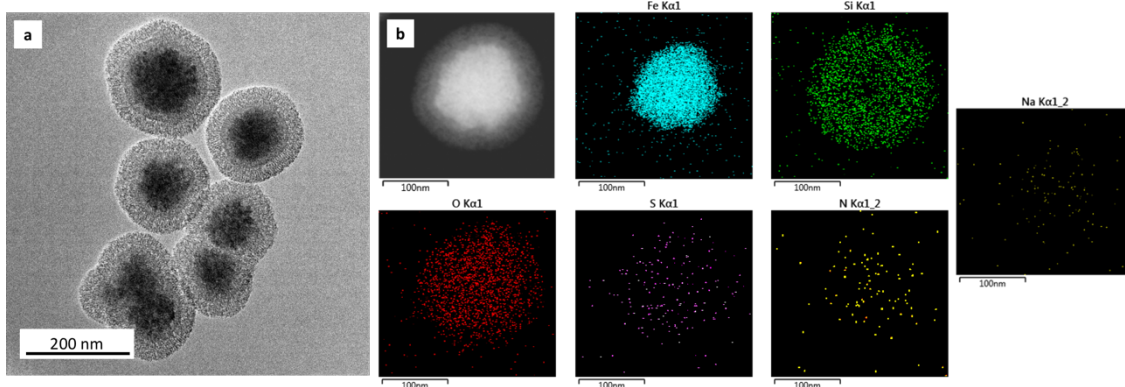


Fig. S15. a) HRTEM of the SPIONs-NCs@MS-MB and b) STEM and mapping of the SPIONs-NCs@MS-MB.

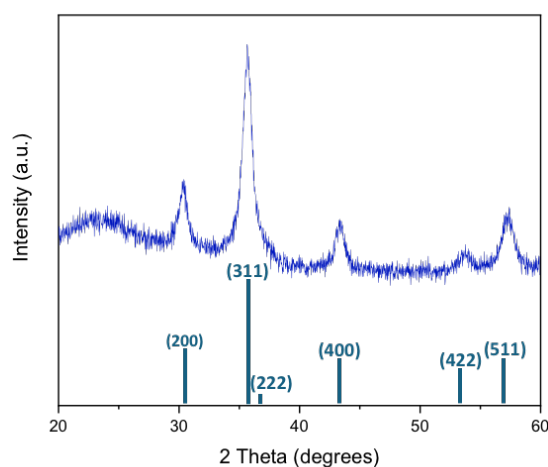


Fig. S16. XRD of the SPIONs-NCs@MS-MB, indexed to magnetite phase,  $\text{Fe}_3\text{O}_4$  (ICDD file No. 19-0629).

Crystallite size was determined by the modified Scherrer method, which reduces errors and gives a constant crystal size for all diffraction peaks.<sup>1,2</sup> The determination was made from 5 reflections ((200), (311), (400), (422), and (511)) whose profiles were fitted to a pseudo-Voigt function. The FWHM associated with the equipment was determined by fitting the peak profiles of a LaB6 pattern to pseudo-Voigt functions. Then, with the corrected values, the crystallite sizes of the SPIONs-NCs (Fig S8) and SPIONs-NCs@MS-MB (Fig. S16) samples are  $10.3 \pm 0.5$  nm and  $11.0 \pm 0.5$  nm, respectively.

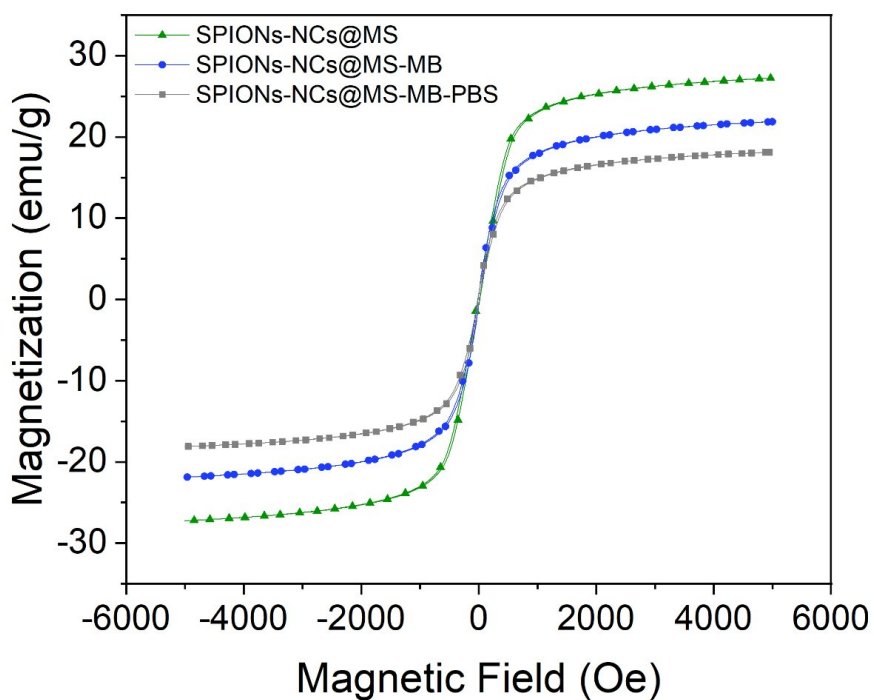


Fig. S17. Magnetization curves of SPIONs-NCs@MS, SPIONs-NCs@MS-MB samples, along with the MB loaded sample after 24h incubation in PBS, designated as SPIONs-NCs@MS-MB-PBS.

#### References

- 1 S. Nasiri, M. Rabiei, A. Palevicius, G. Janusas, A. Vilkauskas, V. Nutalapati and A. Monshi, *Nano Trends*, 2023, **3**, 100015.
- 2 A. Monshi, M. R. Foroughi and M. R. Monshi, *World Journal of Nano Science and Engineering*, 2012, **02**, 154–160.